Nanoscale zero-valent silver and graphene oxide nanoparticles: facile synthesis and characterization

Abstract

We herein report a direct and facile hydrothermal method for the preparation of zero-valent silver nanoparticles using a mixture of ascorbic acid/starch as a reducing agent. The average crystallite size of the prepared Ag^0 nanoparticles was ca. 46.7 nm. The zero-valent silver nano-products were characterized by using FT-IR, FE-SEM, and XRD analyses. In addition, this work shows an improved synthesis of graphene oxide nanoparticles. The average crystallite size of the prepared graphene-oxide nanoparticles was ca. 6.0 nm. The graphene oxide nanoparticles were also characterized by using FT-IR, FE-SEM, and XRD analyses.

Keywords: Silver nanoparticles, Graphene oxide, hydrothermal, ascorbic acid and starch

Introduction

Recently, nanomaterials have been employed in a variety of applications as a result of their sophisticated properties. These materials are distinguished by their exceptional optical properties, small size, unique electronic characteristics, and high reactivity in comparison to bulk materials [1]. A variety of methods are employed to synthesize nanoparticles, including combustion [2], co-precipitation [3], green [4], plasma-enhanced chemical vapor deposition [5], hydrothermal [6], microwave [7], sol-gel methods [8], and chemical reduction methods [9–13].

The attention of scientists and engineers has been extensive due to the unique properties of nanomaterials (1–100 nm materials), such as the small size effect, surface effect, and quantum size effect [14,15]. Nanomaterials possess extraordinary fundamental functions, including high sensitivity, intriguing catalytic activities, and low-temperature sensing, as a result of the small size effect [16]. They possess a high reaction efficiency and a robust adsorption capacity as a result of the surface effect [17]. The quantum size effect has the potential to imbue

nanomaterials with exceptional optical and electronic properties [18]. In the past few decades, a variety of nanomaterials (e.g., nanoparticles, nanowires, nanosheets, nanotubes, nanomembranes, and quantum dots) have garnered significant attention in a variety of fields, including biomedicine, catalysis, energy storage, and sensors, as a result of their distinctive physicochemical properties with respect to their bulk forms [19, 20].

Silver nanoparticles (AgNPs) have received special attention, especially in the field of biomedicine. The broad-spectrum and highly efficacious antimicrobial and anticancer activities of AgNPs are well-known [21]. The hydrothermal method, one of the most critical methods for the production of nanomaterials, has synthesized AgNPs. This method is notable for its ability to produce nanoparticles with narrow size distributions, crystal symmetry, densely sintered powders, and the growth of crystals with ultra-low solubility, all of which are achieved with the use of simple equipment [22]. Carbon is one of the most prevalent elements, which is why carbon materials are more environmentally and biologically favorable than inorganic materials [23]. Carbon nanomaterials, including graphene oxide (GO), are composed of a diverse array of reactive hydroxyl, epoxy, and carboxyl functional groups of oxygen [24].

The thermal and optical properties of GO are exceptional in comparison to those of graphene. The unique characteristics of GO include its ability to disperse easily in water and other solvents as a result of the oxy-functionalities of GO [25–27], its non-cytotoxicity, its adaptable surface, and its low manufacturing costs. Additionally, it possesses effective electron transfer properties that render it a potent fluorescence quencher, making it a valuable new type of nanomaterial for use in biosensors [28, 29].

GO is synthesized from graphite flakes through an oxidative reaction, which results in the sheets being extensively decorated with a variety of oxygen moieties. The modified Hummers method (MHM) [30] and the Hummers method (HM) [31] are the most frequently employed methods for synthesizing graphene oxide. The HM method has been modified to be either a one-step or two-step process. By Chen et al. [32], the one-step MHM method is developed. Also known as the

"Improved Hummers" method, this technique involves the oxidation of graphite without the use of $NaNO_3$. In the two-step modified Hummer's method, the graphite material is initially oxidized by H_2SO_4, $K_2S_2O_8$, and P_2O_5. Hummers' method was then employed to oxidize the pre-oxidized graphite.

"Improved synthesis" of GO was the name of the new method that Tour and colleagues [33] developed. They employed a 9:1 weight ratio of $KMnO_4$ in a mixture of H_2SO_4 and H_3PO_4. In addition, Xu et al. [34] devised an additional approach by decreasing the ratio of $KMnO_4$ to graphite from 3:1 to 1:1. "Mild oxidation" is the term used to describe this method. In the current study, we sought to synthesize silver nanoparticles through hydrothermal synthesis and GO through an enhanced GO synthesis method. Different instruments, including XRD, FT-IR, and FE-SEM, were used to thoroughly characterize the synthesized nanoparticles.

Experimental

Chemicals and reagents

Sigma Aldrich provided us with silver nitrate ($AgNO_3$), ascorbic acid ($C_6H_8O_6$), starch ($C_6H_{10}O_5$), natural graphite, sulphuric acid (H_2SO_4), phosphoric acid (H_3PO_4), potassium per manganate ($KMnO_4$), and hydrogen peroxide (H_2O_2). We used distilled water to prepare all solutions and for cleaning.

Instrumentation

For FT-IR analysis, the Nicolet^{TM} iS50 FT-IR Spectrometer was used in the range of 4000-400 cm^{-1} at room temperature. Field Emission Scanning Electron Microscope (FE-SEM) studies was performed on JEOL model JSM-6390 and X-Ray Diffraction (XRD) studies was performed SHIMADZU model XRD-6000.

Synthesis of silver nanoparticles

The hydrothermal method produced silver nanoparticles (Ag-NPs) by reducing 75 ml of a 0.05 M $AgNO_3$ solution with an ascorbic acid/starch mixture solution. In the experiment, the ascorbic acid:Ag molar ratio was 4, while the starch:Ag molar ratio was 0.3. We autoclaved the mélange at 120 °C. The total volume of the reaction mixture solution was 75 ml. We autoclaved the mélange for four hours. After autoclaving, we filtered the

silver particles through Whatman No. 1 filter paper and then dried them in an electric furnace at 120 °C for 22 hours. In accordance with [35], silver is reduced in aqueous solutions by ascorbic acid.

$$C_6H_8O_6 + 2Ag^+ \rightarrow 2Ag^0 + C_6H_6O_6 + 2H^+$$

Synthesis of graphene oxide

We poured a 9:1 mixture of concentrated H_2SO_4/H_3PO_4 (360:40 ml) into a mixture of graphite powder (3 g) and $KMnO_4$ (18 g), which produced a mild exotherm at 35–40 °C. Then the reaction mixture was warmed to 50 °C and stirred for 6 hours. The mixture was cooled to room temperature and poured onto ice (~400 ml) with 30% H_2O_2 (3 ml) until the solution turned yellow. We centrifuged the solution at 4000 rpm and removed the supernatant. We then washed the remaining solid material in succession with 200 mL of water, 200 ml of 30% HCl, and 200 ml. We centrifuged the mixture at 4000 rpm after each wash and decanted away the supernatant. We vacuum-dried the solid yield at 50 °C [36]. The structure of GO is presented in Fig. 1.

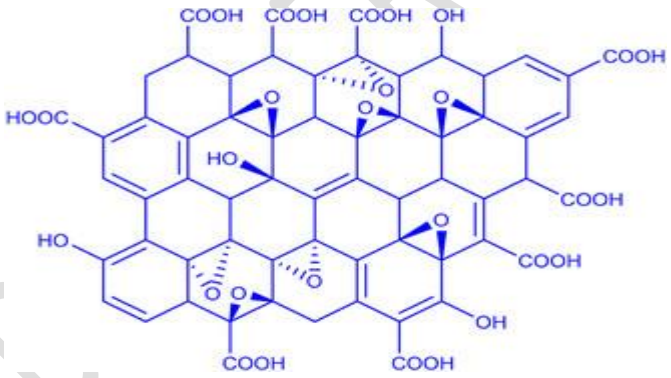

Figure. 1. *Structure of graphene oxide [34].*

Results and discussion

Characterization of silver nanoparticales

XRD pattern

Figure 2 illustrates the XRD patterns of Ag-NPs. As you look at the XRD pattern, the peaks at 38.12º, 44.31º, 64.46º, and 77.41º show the (111), (200), (220), and (311) hkl planes of the silver nanoparticles in the FCC lattice. The synthesized Ag-NPs have an average crystallite size of 46.7 nm.

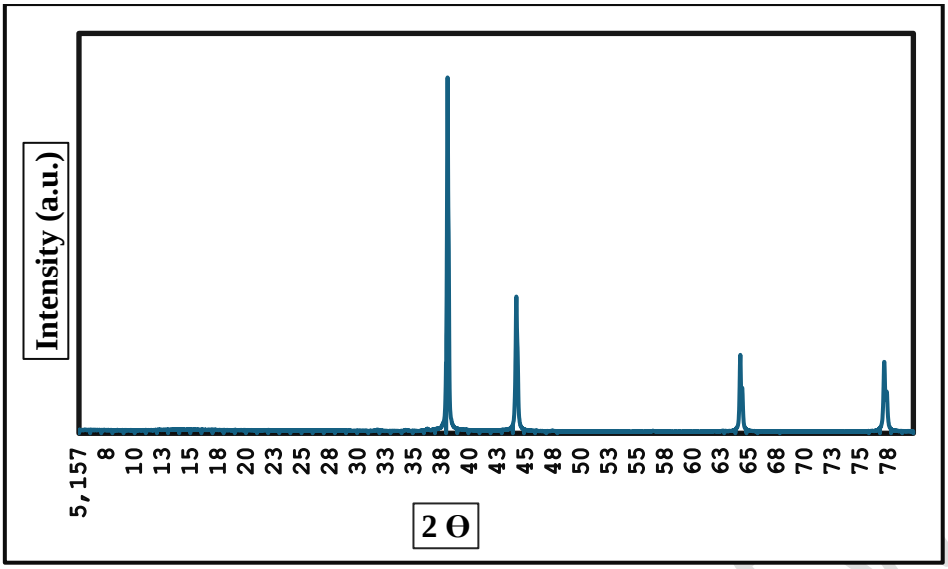

Figure. 2. *XRD Pattern of Ag-NPs*

FESEM images

The FE-SEM images of the synthesized Ag-NPs were predominantly spherical in shape (Fig. 3).

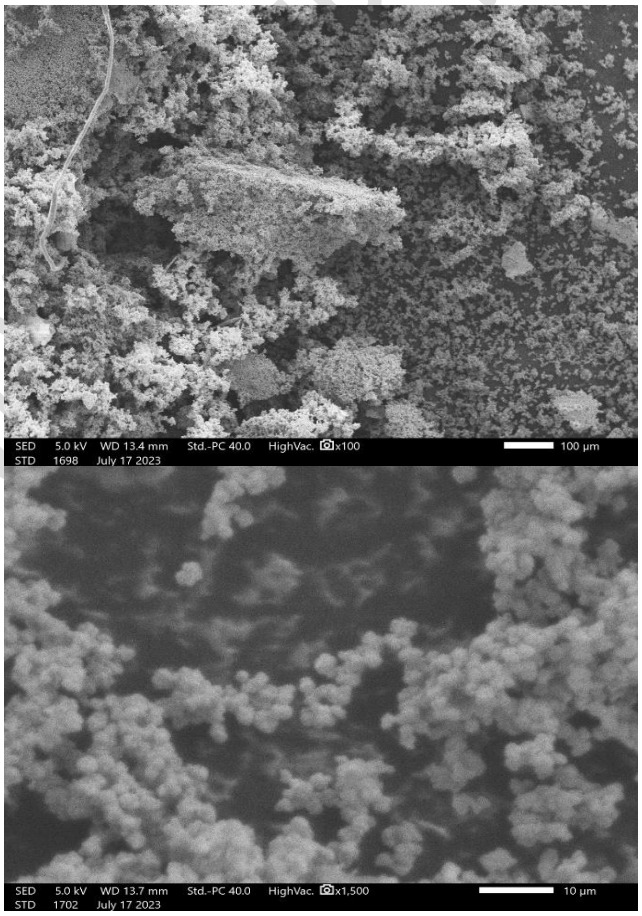

Figure. 3. *FESEM images of Ag-NPs*

Characterization of graphene oxide nanoparticles

XRD pattern

Figure 4 illustrates the XRD patterns of GO nanoparticles. The intense peak at 2θ of 10.48° in the case of graphene oxide is indicative of the (001) plane, which is the primary characteristic of GO. This suggests that the "improved synthesis" method of GO is effectively used to prepare GO with an average crystallite size of 6 nm through the oxidation of graphite.

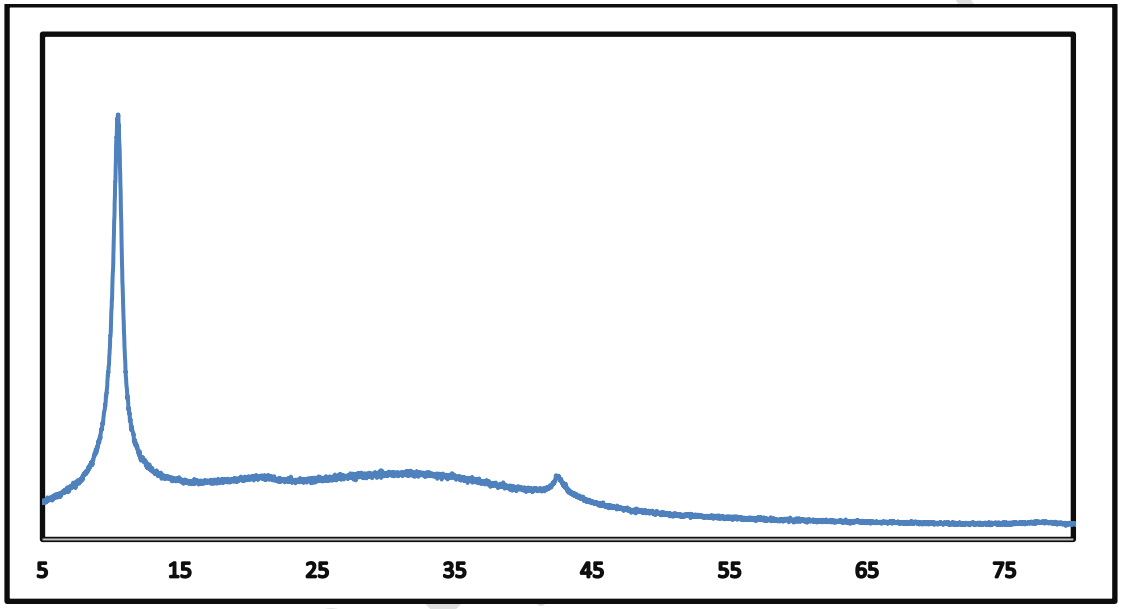

Figure. 4. *XRD Pattern of GO*

FESEM images

We further evaluated the morphology of GO using FE-SEM. The graphene oxide (GO) had a two-dimensional structure with a stratified distribution that stacked together in a flocculent manner. The surface was relatively flat (Fig. 5).

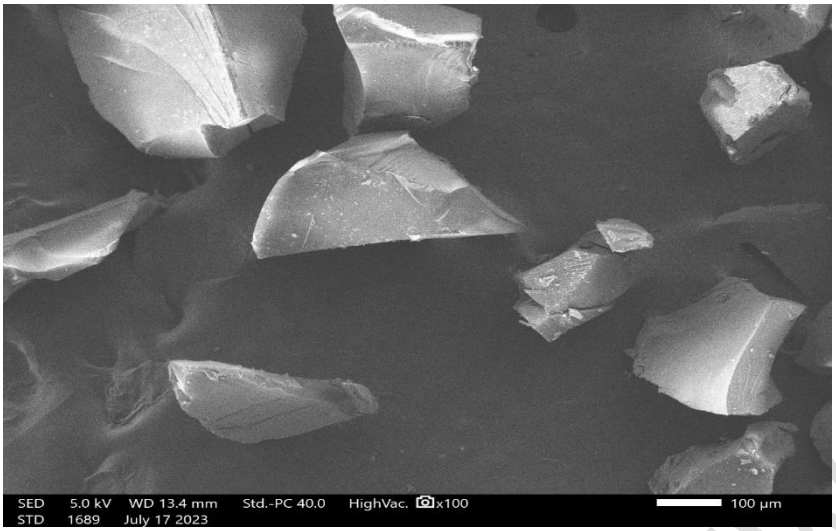

Figure. 5. *FE-SEM image of GO*

FT-IR spectroscopy

FT-IR spectroscopy is a powerful tool that can be used to describe the presence of different functional groups in graphene oxide, including functional groups that contain oxygen. The FT-IR spectrum (Fig. 6) confirmed the effective oxidation of the graphite. We identified certain functional groups, including O-H, C-OH, COOH, and C-O [37, 38]. The carboxyl O-H stretching mode is responsible for the broad peak in the IR spectrum of GO, which is located between 3500 cm^{-1} and 2500 cm^{-1} . The presence of absorbed water molecules and alcohol groups is the reason for the absorption peaks that correspond to O-H stretching (a peak at approximately 3400 cm^{-1}) that is superimposed on the OH stretch of carboxylic acid. The asymmetric CH_2 stretching of GO is responsible for the IR peaks at 2927 cm^{-1} , while the peak at 1600 cm^{-1} is attributed to C=C strains from the unoxidized graphitic domain. The peak at approximately 1700 cm^{-1} is attributed to the C=O stretch of the carboxyl group, while the peak at 1220 cm-1 corresponds to the C-OH stretch of the alcohol group. The peak at 1020 cm^{-1} is attributed to the C-O stretching vibrations of the C-O-C.

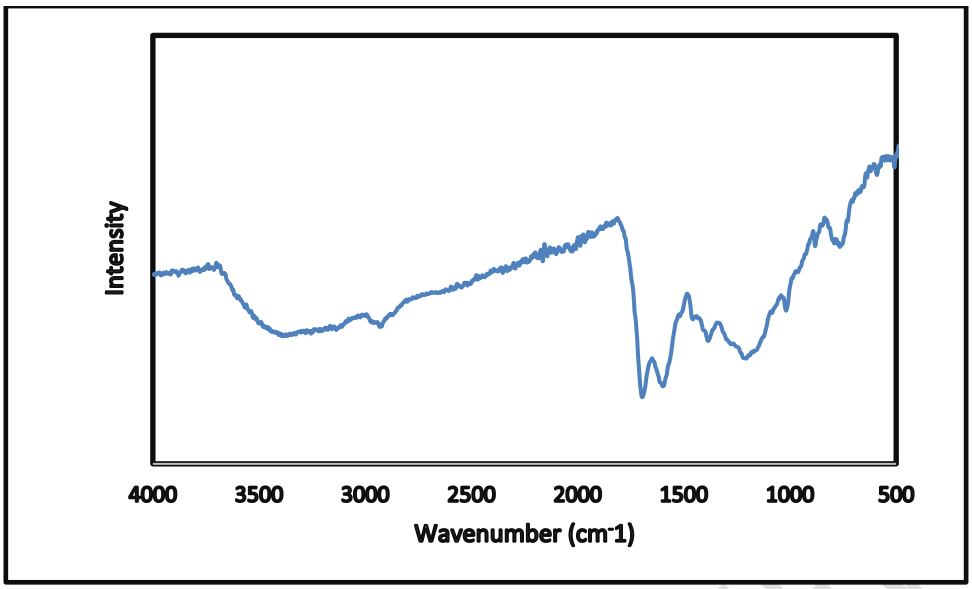

Figure . 6. *FT-IR spectra of GO*

Conclusion

We employed the hydrothermal method to create silver nanoparticles by combining silver nitrate with starch as a surfactant. We utilized the "improved synthesis" procedure to produce GO from graphite. We employed a diverse array of techniques to characterize the nanoparticles that were obtained, such as Fourier transform infrared analysis (FTIR), x-ray particle diffraction (XRD), and field emission scanning electron microscopy (FE-SEM). The average crystallite size of Ag-NPs and GO was 46.7 nm and 6 nm, respectively.

References

1. N. Baig, I. Kammakakam, and W. Falath, *Nanomaterials: a review of synthesis methods, properties, recent progress, and challenges.* Materials Advances, 2021. **2**(6): p. 1821-1871.
2. F. Quan, A. mao, M. ding, S. Ran, J. Wang, G. Yang, and Y. Yan, *Combustion synthesis and formation mechanism of silver nanoparticles.* International Journal of Materials Research, 2018. **109**(8): p. 751-755.

3. Y. Dasaradhudu, and M. Arunachalam Srinivasan, *Synthesis and characterization of silver nano particles using co-precipitation method.* Materials Today: Proceedings, 2020. **33**: p. 720-723.
4. D. K. Chandrasekharan, p. k. khanna, t. v. kagiya, and c. k. k. nair, *Synthesis of nanosilver using a vitamin C derivative and studies on radiation protection.* Cancer Biother Radiopharm, 2011. **26**(2): p. 249-57.
5. Y. Hayashi, H. Sawada, and H. Takagi, *Growth of Vertically Aligned Carbon Nanotubes by RF-DC Plasma Chemical Vapor Deposition*. 2011.
6. M. Mostafa, *Synthesis of nanosilver by the hydrothermal method and its application for radioiodine sorption from alkaline solution.* Journal of Radioanalytical and Nuclear Chemistry, 2015. **304**(3): p. 1153-1162.
7. M.N. Nadagouda, T.F. Speth, and R.S. Varma, *Microwave-Assisted Green Synthesis of Silver Nanostructures.* Accounts of Chemical Research, 2011. **44**(7): p. 469-478.
8. A. Tavakol, M. Sohrabi, and A. Kargari, *A review of methods for synthesis of nanostructured metals with emphasis on iron compounds.* Chemical Papers, 2007. **61**(3): p. 151-170.
9. R. Singh, V. Misra, and R.P. Singh, *Removal of hexavalent chromium from contaminated ground water using zero-valent iron nanoparticles.* Environ Monit Assess, 2012. **184**(6): p. 3643-51.
10. Y. Zhuang, S.Ahn, A.L.Seyfferth, Y.Masue-slowey, S.Fendorf, and R. G. Luthy, *Dehalogenation of polybrominated diphenyl ethers and polychlorinated biphenyl by bimetallic, impregnated, and nanoscale zerovalent iron.* Environ Sci Technol, 2011. **45**(11): p. 4896-903.
11. Yadav, A., Shreya, & Puri, N. K. (2022, November). Preliminary observations of synthesized WS2 and various synthesis techniques for preparation of nanomaterials. In *Advances in Manufacturing Technology and Management: Proceedings of 6th International Conference on Advanced Production and Industrial Engineering (ICAPIE)—2021*. 546-556.
12. Phogat, P., Jha, R., & Singh, S. (2024). Carbon nanospheres-induced enhanced capacitive dynamics in C/WS_2/WO_3 nanocomposites for high-performance electrochemical capacitors. Materials Science and Engineering: B, **304**, 117390.
13. Phogat, P., Jha, R., & Singh, S. (2024). Synthesis of Novel ZnO Nanoparticles with Optimised Band Gap of 1.4 eV for High-Sensitivity Photo Electrochemical Detection. Materials Today Sustainability, 100823.

14. c. Li, H. Yu, Z. Du, and T. Wang, *Low-temperature sensing and high sensitivity of ZnO nanoneedles due to small size effect.* Thin Solid Films, 2009. **517**: p. 5931-5934.
15. S. Sarkar, E. Guibal, F.Quignard, and A. K. Sengupta, *Polymer-supported metals and metal oxide nanoparticles: synthesis, characterization, and applications.* Journal of Nanoparticle Research, 2012. **14**(2): p. 715.
16. G. Wang, Y. Wang, L. Chen, and J. Choo, *Nanomaterial-assisted aptamers for optical sensing.* Biosensors and Bioelectronics, 2010. **25**(8): p. 1859-1868.
17. Y. Wang, K. Qu, L. Tang, Z. Li, E.Moore, X. Zeng, Y. Liu, and J. Li, *Nanomaterials in carbohydrate biosensors.* TrAC Trends in Analytical Chemistry, 2014. **58**.
18. G. Ghasemzadeh, M. Momenpour, F. Omidi, M. R. Hosseini, M. Ahani, A. *Barzegari* Applications of nanomaterials in water treatment and environmental remediation. Frontiers of Environmental Science & Engineering, 2014. 8(4): p. 471-482.
19. Q. Li, L. S. Wang, B. Y. Hu, and C. Yang, *Preparation and characterization of NiO nanoparticles through calcination of malate gel.* Materials Letters - MATER LETT, 2007. **61**: p. 1615-1618.
20. Y. Ju-Nam, and J.R. Lead, *Manufactured nanoparticles: an overview of their chemistry, interactions and potential environmental implications.* Sci Total Environ, 2008. **400**(1-3): p. 396-414.
21. J. Zhao, Y. Zou, X. Zou, T, Bai, Y. Liu, R. Gao, d. Wang, and G.-D. Li, *Self-template construction of hollow Co3O4 microspheres from porous ultrathin nanosheets and efficient noble metal-free water oxidation catalysts.* Nanoscale, 2014. **6**(13): p. 7255-7262.
22. L. Xu, Y. -Y. Wang, J. Huang, C. -Y. Wang, H. Xie, *Silver nanoparticles: Synthesis, medical applications and biosafety.* Theranostics, 2020. **10**(20): p. 8996-9031.
23. K. Byrappa, and T. Adschiri, *Hydrothermal technology for nanotechnology.* Progress in Crystal Growth and Characterization of Materials, 2007. **53**(2): p. 117-166.
24. C, Chung, Y. -K. Kim, D. Shin, S. -R. Ryoo, B. H. Hong, and D. -H. Min, *Biomedical applications of graphene and graphene oxide.* Acc Chem Res, 2013. **46**(10): p. 2211-24.
25. D. R. Dreyer, S. Park, C. W. Bielawski, and R. S. Ruoff, *The chemistry of graphene oxide.* Chemical Society Reviews, 2010. **39**(1): p. 228-240.
26. A. Kundu, R. K. Layek, A. Kuila, and A. K. Nadi, *Highly Fluorescent Graphene Oxide-Poly(vinyl alcohol) Hybrid: An*

Effective Material for Specific Au3+ Ion Sensors. ACS Applied Materials & Interfaces, 2012. **4**(10): p. 5576-5582.
27. Y. Liu,C. Tian, B. Yan, Q. Lu, Y. Xie, J. Chen, R. Gupta, Z. Xu, S. M. Kuznicki, Q. Liu, and H. Zeng, *Nanocomposites of graphene oxide, Ag nanoparticles, and magnetic ferrite nanoparticles for elemental mercury (Hg0) removal.* RSC Advances, 2015. **5**(20): p. 15634-15640.
28. J. Huang, L. Zhang, B. Chen, N. Ji, F. Chen, Y. Zhang, and Z. Zhang, *Nanocomposites of size-controlled gold nanoparticles and graphene oxide: Formation and applications in SERS and catalysis.* Nanoscale, 2010. **2**(12): p. 2733-2738.
29. J. Liang, R. Wei, S. He, Y. Liu, L. Guo, and L. Li, *A highly sensitive and selective aptasensor based on graphene oxide fluorescence resonance energy transfer for the rapid determination of oncoprotein PDGF-BB.* Analyst, 2013. **138**(6): p. 1726-1732.
30. M. Li, S. Guo, N. Wu, and X. Zhou, *Detection of lead (II) with a "turn-on" fluorescent biosensor based on energy transfer from CdSe/ZnS quantum dots to graphene oxide.* Biosensors and Bioelectronics, 2013. **43**: p. 69-74.
31. Y. Wang, Y. Li, L. Tang, J. Lu, and J. Li, *Application of graphene-modified electrode for selective detection of dopamine.* Electrochemistry Communications, 2009. **11**: p. 889-892.
32. *N. I. Kovtyukhova, P. J. Ollivier, B. R. Martin, T. E. Mallouk, S. A. Chizhik, E. V. Buzaneva, and* A. D. Gorchinskiy, *Layer-by-Layer Assembly of Ultrathin Composite Films from Micron-Sized Graphite Oxide Sheets and Polycations.* Chemistry of Materials, 1999. **11**(3): p. 771-778.
33. J. Chen, B. Yao, C. Li, and G. Shi, *An improved Hummers method for eco-friendly synthesis of graphene oxide.* Carbon, 2013. **64**: p. 225-229.
34. D. C. Marcano, D. V. Kosynkin, J. M. Berlin, A. Sinitskii, Z. Sun, A. Slesarev, L. B. Alemany, W. Lu, and J. M. Tour, *Improved Synthesis of Graphene Oxide.* ACS Nano, 2010. **4**(8): p. 4806-4814.
35. Y. Xu, K. Sheng, C. Li, and G. Shi, *Highly conductive chemically converted graphene prepared from mildly oxidized graphene oxide.* Journal of Materials Chemistry, 2011. **21**(20): p. 7376-7380.
36. D. Singha, N. Barman, and K. Sahu, *A facile synthesis of high optical quality silver nanoparticles by ascorbic acid reduction in reverse micelles at room temperature.* Journal of Colloid and Interface Science, 2014. **413**: p. 37-42.

37. K. Gerani, H. Mortaheb, and B. Mokhtarani, *Enhancement in performance of sulfonated polyether sulfone cation exchange membrane by functionalized graphene oxide Nano sheets*. 2015.
38. B. Zhang, and D. Zhang, *Aqueous colloids of graphene oxide nanosheets by exfoliation of graphite oxide without ultrasonication.* Bulletin of Materials Science, 2011. **34**(1): p. 25-28.

Elamin NY, Eltom E, Ramadan R. Green Synthesis of Lead Oxide Nanoparticles, Characterization and Adsorption Study for Removal of Malachite Green Dye. Asian J. Appl. Chem. Res. [Internet]. 2023 Mar. 10 [cited 2024 May 25];13(2):16-22. Available from: https://journalajacr.com/index.php/AJACR/article/view/239

Sogbochi E, Nonviho G, Bokossa HKJ, Agodji C, Sohounhloue DCK. Mechanism and Kinetic Studies of the Adsorption of Congo Red on Three Adsorbent Materials. Chem. Sci. Int. J. [Internet]. 2024 Mar. 26 [cited 2024 May 25];33(3):22-34. Available from: https://journalcsij.com/index.php/CSIJ/article/view/892

Milosavljevic V, Mitrevska K, Adam V. Benefits of oxidation and size reduction of graphene/graphene oxide nanoparticles in biosensing application: Classification of graphene/graphene oxide nanoparticles. Sensors and Actuators B: Chemical. 2022 Feb 15;353:131122.